Applied Physics Letters PERSPECTIVE scitation.org/journal/apl

Perspectives on high resolution microvascular imaging with contrast ultrasound

Cite as: Appl. Phys. Lett. **116**, 210501 (2020); doi: 10.1063/5.0012283
Submitted: 29 April 2020 · Accepted: 30 April 2020 ·
Published Online: 26 May 2020

Thomas M. Kierski and Paul A. Dayton[a)]

AFFILIATIONS

The Joint Department of Biomedical Engineering, The University of North Carolina at Chapel Hill and North Carolina State University, Campus Box 7575, Chapel Hill, North Carolina 27599, USA

[a)]Author to whom correspondence should be addressed: padayton@email.unc.edu

ABSTRACT

Recent developments in contrast enhanced ultrasound have demonstrated a potential to visualize small blood vessels *in vivo*, unlike anything possible with traditional grayscale ultrasound. This Perspective article introduces microvascular imaging strategies and their underlying technology.

Ultrasound is distinguished among the common biomedical imaging modalities by its relatively low cost, high temporal and spatial sampling frequencies, safety, accessibility, and portability. Ultrasonography has long been used by clinicians for investigating organs such as the kidney,[1] heart,[2] liver,[3] spleen,[4] prostate,[5] thyroid,[6] and others using conventional B-scan imaging. In addition to these large anatomical features, it is also possible to noninvasively measure the mechanical properties of tissues, blood dynamics, and molecular signaling using elastography,[6] Doppler imaging,[7] and molecular imaging,[8,9] respectively. While B-scan and Doppler imaging are commonplace in many clinics, it is important to note their limitations. The spatial resolutions of these approaches are fundamentally diffraction-limited, which means that higher frequencies are necessary to image smaller targets. Many biological tissues have attenuative properties that grow exponentially as the frequency is increased.[10] Therefore, high-frequency imaging is generally restricted to shallow and superficial targets because of the poor signal to noise ratio (SNR) at depth.

However, there are numerous microscopic targets of interest in the body. Ailments such as cancer, chronic kidney disease, atherosclerosis, and others exhibit characteristic microvascular structures that are part of their pathophysiological fingerprints.[11–13] For example, one of the hallmarks of cancer is a network of densely packed and highly tortuous vessels that invade rapidly to feed a tumor as it grows.[11] Though these features may contain important diagnostic information, they cannot be easily quantified via conventional ultrasound methods because of the resolution and/or SNR. In light of these shortcomings, recent research has focused on developing new hardware, pulse sequences, and signal processing methods for scanning micro-sized blood vessels.

The sensitivity of ultrasonography to blood can be improved significantly by administering microbubble contrast agents (MBs), which are spheres that normally range between 1 and 5 μm in diameter with a gas core and a lipid or protein shell. The acoustic impedance of a microbubble is very different than that of biological tissue; hence, these agents strongly reflect acoustic waves. Because MBs are similar to erythrocytes in size, they are distributed by circulation mechanics throughout the blood pool. In addition to being excellent reflectors *in vivo*, microbubbles are exceedingly nonlinear compared to biological tissues. For conventional diagnostic imaging, a pulse with some bandwidth is transmitted into the body, and most of the backscattered echoes have a frequency content that is centered at the fundamental or second harmonic of the transmitted waveform.[14] When sonicated at or near its resonant frequency, a contrast agent exhibits a broadband response with many harmonics present above the fundamental.[15,16] The third and higher harmonics are typically referred to as "super harmonics."[17]

One approach that makes use of this strongly nonlinear acoustic behavior is known as acoustic angiography.[18] Briefly, a super-wideband probe is used to excite an MB contrast agent with a pulse at or near its resonant frequency, and the super harmonic echoes are recorded. Compared to MBs, the acoustic backscatter from the tissue is narrowband. Hence, the super harmonic frequency band is dominated by MB echoes. This technique has the advantage of a high contrast to tissue ratio (CTR) due to the large separation of the tissue and higher order microbubble harmonics, and a high resolution based on

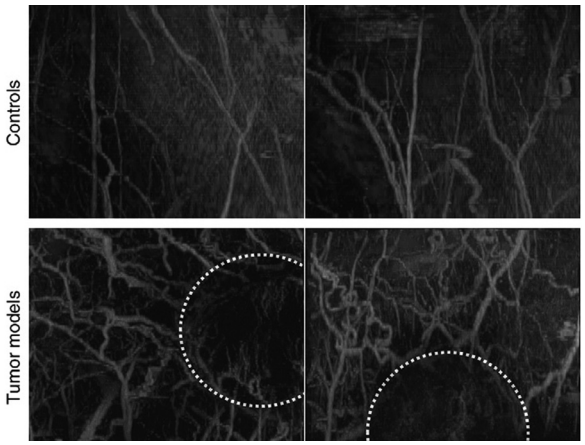

FIG. 1. Application of microvascular ultrasound imaging to oncology. Acoustic angiography illustrates the presence of tortuosity and high vascular density due to tumor-associated angiogenesis (bottom) vs lack thereof in healthy tissue (top). The dotted lines indicate the approximate tumor locations. Partially Reproduced with permission from Gessner *et al.*, Radiology, **264**, 733 (2012).

the high receive frequency. Because it utilizes a low-frequency transmitting signal and then a high-frequency receiving signal, it is possible to image targets at greater depths than is possible with a two-way high-frequency scheme. Though this approach is diffraction-limited, it can resolve vessels on the order of 100 μm in diameter at 1–2 cm, and importantly, it retains the benefit of real-time imaging.

Acoustic angiography can provide high resolution vascular maps without tissue clutter, and has been useful for quantifying the vascularity of preclinical targets such as subcutaneous tumors[19] and organoid models[20] (Fig. 1). However, the availability of this technique is limited because it requires super-wideband transducers, usually fabricated with separate transmitting and receiving elements.[21] To date, preclinical devices have been optimized for imaging at depths of approximately 1–2 cm, which excludes most human cancers. It is important to note, however, that this is not the physical limit of super harmonic imaging. Recent work in dual-frequency transducer design has resulted in impressive contrast sensitivity as deep as 3 cm *in vivo* transmitting and receiving at 2 and 20 MHz, respectively.[22,23] Similarly, further reduction of the frequencies used in super harmonic imaging can further improve the penetration depth at the expense of resolution. Continued development of dual frequency array technology for acoustic angiography is in progress to improve the depth of field, sensitivity to contrast, and frame rate for clinical applications (Table I).

More recently, a technique known as ultrasound localization microscopy (ULM) has been developed that can achieve even higher resolutions than acoustic angiography.[24] This is a super resolution technique analogous to fluorescence photoactivation localization microscopy,[25] which means that it improves upon the diffraction-limited resolution fundamental to coherence-based imaging systems. Though there are many variations to ULM documented in the literature, the general approach can be described with the steps below:

(1) Data collection: microbubbles are administered intravenously and a series of data is acquired. Hundreds to thousands of images are collected, normally at large frame rates greater than 100 Hz.
(2) Contrast echo separation: microbubble echoes are isolated in preparation for contrast localization. For fundamental B-mode imaging *in vivo*, microbubble signals are overlapped with tissue backscatter as well as noise. Spatiotemporal filters, such as those based on singular value decomposition (SVD) or nonlocal means, have been utilized by different groups[26–28] for this problem. In short, these methods distinguish bubbles from other sources by differences in their spatiotemporal coherence. Another common approach is to capitalize on the nonlinear response of MBs to separate them from the tissue using techniques such as pulse inversion,[29] amplitude modulation,[30] and contrast pulse sequences.[31] Harmonic imaging sequences are often combined with slow time filters to improve the CTR for moving bubbles, especially when stationary imaging artifacts are present.
(3) Microbubble localization: once microbubbles are isolated, their positions are estimated on a sub-wavelength grid. By processing

TABLE I. Comparison of various angiographic imaging modalities. Here, "resolution" refers to the smallest vessel diameter reconstructed with a given technique. PAT: photoacoustic tomography, OCT-A: optical coherence tomography angiography, MRA: magnetic resonance angiography, MCT-A: micro-CT angiography, DSA: digital subtraction angiography, AA: acoustic angiography, and ULM: ultrasound localization microscopy.

	Resolution	SNR	Max depth	Scan time	Image volume
PAT (2 MHz transducer)[43]	370 μm	60 dB	50 mm	120–240 s	1×10^5 mm^3
PAT (40 MHz transducer)[44]	50 μm	32.5 dB	3.1 mm	20 min	1×10^3 mm^3
OCT-A[45]	5 μm	20 dB	3 mm	<10 s	1×10^1–1×10^2 mm^3
MRA (9.4 Tesla)[46]	60 μm	34 dB	>100 mm	58 min	1×10^3–5×10^3 mm^3
MCT-A[46]	50 μm	25 dB	>100 mm	20–40 s	1×10^2–1×10^3 mm^3
DSA[46]	40 μm	20 dB	>100 mm	<1 s	[b]
AA[47,48]	150 μm	25 dB	<40 mm	120 s	1–2 $\times 10^4$ mm^3
ULM (15 MHz linear array)[26]	15 μm	[a]	12 mm	150 s	[b]
ULM (9 MHz matrix array)[33]	50 μm	[a]	30 mm	12 s	1×10^3–1×10^4 mm^3

[a]Not reported.
[b]Not applicable for 2D imaging modalities.

many acquisitions in this way, a map of the vasculature is constructed over time. An excellent comparison of many localization methods has been provided by Jeffries *et al.*[32]

A very active area of research that will impact the way that data is collected for ULM is ultrafast volumetric imaging. Many of the seminal studies in the field utilized linear array transducers therefore the first volumetric ULM scans were generated by translating a transducer in the elevational dimension between acquisitions. This approach produces elevational resolutions orders of magnitude larger than the axial and lateral counterparts. Additionally, the time necessary to acquire a single volume is prohibitively large for most clinical scenarios. Matrix arrays can be fully sampled, such as in Heiles *et al.*,[33] but these are typically restricted to small-aperture imaging in light of the large channel counts required to fully populate a larger aperture. An important and active area of research is focused on the development of novel matrix arrays that can achieve a comparable imaging quality with a reduced data bandwidth. For example, sparse[34] and row-column addressed arrays[35] are two approaches that may allow for ultrafast volumetric imaging at depth by increasing the aperture size and decreasing the channel count.

One of the greatest challenges for clinical translation of ultrasound localization microscopy to the clinic is physiological motion. As was mentioned previously, many ULM processing pipelines utilize complex spatiotemporal filters to separate microbubble echoes from background signals, but the performance of these methods is degraded in the presence of motion artifacts as a result of overlapping spatiotemporal features of contrast and tissue. For very static targets such as the brain, these techniques might still be appropriate, but very dynamic targets such as the heart are displaced by lengths orders of magnitude greater than the vessels of interest. For this reason, it is possible that super harmonic imaging approaches such as acoustic angiography might become highly useful for ultrafast imaging of these organs, particularly because the loss of resolution at lower frequencies can be readily recovered by ULM while the discrimination between the flowing microbubbles and the moving tissue is preserved by frequency separation. To date, pulse inversion and super harmonic imaging have produced promising results for organs such as the kidney[28,36,37] (see Fig. 2), but more research is required to develop and validate robust motion correction schemes that do not create or destroy the vascular structure in reconstructed images. A variety of rigid[36,38] and non-rigid[37,39] correction frameworks have been presented in recent years, and the discussion remains open as to which approaches are the most efficacious.

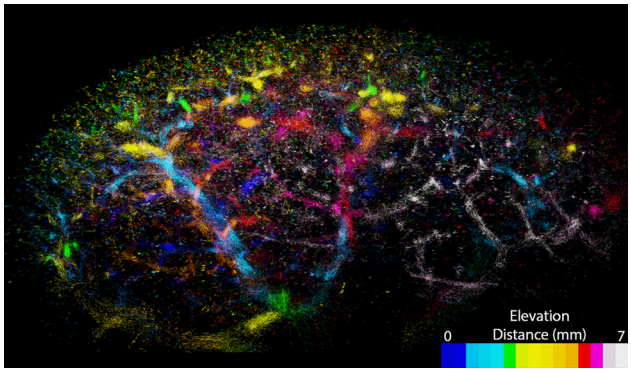

FIG. 2. A 3D ULM image of a rodent kidney generating using super harmonic imaging. The distance from the observer is color-coded according to the map provided. Reconstructed from data from Kierski *et al.*[37]

Slow flow is also a challenge for some current implementations of ULM. Filters based on SVD, for example, are not sensitive to bubbles which move very slowly relative to the surrounding tissue.[37] This phenomenon suggests that these filters impose an artificial cap on the resolution of ULM imaging because contrast agents move very slowly in the smallest capillaries.[40,41] This notion is supported by the fact that literature is yet to demonstrate success in the imaging of microvessels at theoretical resolution limits (e.g., 1.8 μm for a 7 MHz linear array with a 30 mm aperture width).[42] Slow flow sensitivity will be especially important for the development of super resolution molecular imaging techniques, where the goal is to localize targeted microbubbles *in vivo*. As it currently stands, demonstration of detection and localization of adherent targeted bubbles in the presence of freely circulating contrast is yet to be achieved.

Artificial intelligence holds great promise for upending the entire ULM imaging pipeline. Van Sloun and colleagues have demonstrated the feasibility of localizing bubbles in beamformed images using deep convolutional neural networks.[49] It is possible that end-to-end deep learning approaches will play a critical role in the clinical translation of this imaging modality by allowing the radio frequency data to be processed in real time to accumulate bubble positions. This sort of processing will eliminate the need to save extremely large datasets for offline processing and has the potential to improve acquisition times by localizing more bubbles per image than can be achieved by conventional approaches.

Sparse element configurations are especially interesting considering recent work in compressed sensing applied to ultrasound. It is known that the increasing element count can reduce the impact of clutter for challenging targets *in vivo*, but it is possible that deep learning approaches such as those presented in Xiao and colleagues[50] will be appropriate for augmenting the performance of ultrafast volumetric imaging in the clinic.

Deep learning also holds great promise for aiding clinicians in the interpretation of ULM images. ULM images provide an incredibly rich and complex dataset, combining 3D morphological information with velocimetry in many cases. Computer-aided diagnosis developed on deep neural networks may be crucial for the adoption of these techniques by providing physicians an insight into the nuances of each dataset. This approach might prove especially useful once molecular imaging methods are combined with ULM, as this will add yet another feature space for analysis.

Microvascular imaging with ultrasound is a promising technique for qualitative and quantitative assessment of a variety of organs and diseases. While many groups have published impressive images of various targets in preclinical models, research is ongoing to investigate the clinical impact of these technologies. Further progress in areas such as ultrafast volumetric imaging and deep learning will be crucial for overcoming the challenges associated with slow flow, physiological motion, and imaging time.

Support for our research in ultrasonic microvascular imaging has been provided by the National Institutes of Health (Nos. R01CA170665, R01CA170665S1, R01EB026897, R01CA189479, R44CA165621, R01EB015508, R01EB025149, and 1R01CA220681),

DOD No. W81XWH-12–1-0303, as well as the Lineberger Comprehensive Cancer Center. The authors appreciate the contributions of the many collaborators from the University of North Carolina at Chapel Hill, the University of Toronto, North Carolina State University, FUJIFILM Visualsonics, Inc., and Kitware, Inc. who have collaborated on this work. P.A.D. declares that he is a co-inventor on patents describing microvascular imaging technologies and a co-founder of SonoVol, Inc, which has licensed some of these technologies.

DATA AVAILABILITY

Data sharing is not applicable to this article as no new data were created or analyzed in this study.

REFERENCES

[1]M. L. Robbin, M. E. Lockhart, and R. G. Barr, Radiol. Clin. North Am. **41**, 963 (2003).
[2]S. C. Cheng, T. C. Dy, and S. B. Feinstein, Am. J. Cardiol. **81**, 41G (1998).
[3]S. R. Wilson and P. N. Burns, Semin. Liver Dis. **21**, 147 (2001).
[4]P. Peddu, M. Shah, and P. S. Sidhu, Clin. Radiol. **59**, 777 (2004).
[5]E. J. Halpern, Rev. Urol. **8**(1), S29 (2006).
[6]F. Sebag, J. Vaillant-Lombard, J. Berbis, V. Griset, J. F. Henry, P. Petit, and C. Oliver, J. Clin. Endocrinol. Metab. **95**, 5281 (2010).
[7]C. Demene, J. Baranger, M. Bernal, C. Delanoe, S. Auvin, V. Biran, M. Alison, J. Mairesse, E. Harribaud, M. Pernot, M. Tanter, and O. Baud, Sci. Transl. Med. **9**, 1 (2017).
[8]R. Gessner and P. A. Dayton, Mol. Imaging Off. J. Soc. Mol. Imaging **9**, 117 (2010).
[9]J. K. Tsuruta, N. Klauber-DeMore, J. Streeter, J. Samples, C. Patterson, R. J. Mumper, D. Ketelsen, and P. Dayton, PLoS One **9**, e86642 (2014).
[10]S. A. Goss, L. A. Frizzell, and F. Dunn, Ultrasound Med. Biol. **5**, 181 (1979).
[11]D. Hanahan and R. A. Weinberg, Cell **144**, 646 (2011).
[12]D. A. Long, J. T. Norman, and L. G. Fine, Nat. Rev. Nephrol. **8**, 244 (2012).
[13]S. Carlier, I. A. Kakadiaris, N. Dib, M. Vavuranakis, C. Stefanadis, S. M. O'Malley, C. J. Hartley, R. Metcalfe, R. Mehran, E. Falk, K. Gul, and M. Naghavi, Curr. Atheroscler. Rep. **7**, 164 (2005).
[14]J. D. Thomas and D. N. Rubin, J. Am. Soc. Echocardiogr. **11**, 803 (1998).
[15]N. de Jong, R. Cornet, and C. T. Lancée, Ultrasonics **32**, 447 (1994).
[16]N. de Jong, R. Cornet, and C. T. Lancée, Ultrasonics **32**, 455 (1994).
[17]A. Bouakaz, S. Frigstad, F. J. Ten Cate, and N. De Jong, Medicine **28**, 59 (2002).
[18]R. C. Gessner, C. B. Frederick, F. S. Foster, and P. A. Dayton, Int. J. Biomed. Imaging **2013**, 1.
[19]S. E. Shelton, Y. Z. Lee, M. Lee, E. Cherin, F. S. Foster, S. R. Aylward, and P. A. Dayton, Ultrasound Med. Biol. **41**, 1896 (2015).
[20]A. Wahl, C. De, M. Abad Fernandez, E. M. Lenarcic, Y. Xu, A. S. Cockrell, R. A. Cleary, C. E. Johnson, N. J. Schramm, L. M. Rank, I. G. Newsome, H. A. Vincent, W. Sanders, C. R. Aguilera-Sandoval, A. Boone, W. H. Hildebrand, P. A. Dayton, R. S. Baric, R. J. Pickles, M. Braunstein, N. J. Moorman, N. Goonetilleke, and J. Victor Garcia, Nat. Biotechnol. **37**, 1163 (2019).
[21]K. Martin, B. Lindsey, J. Ma, M. Lee, S. Li, F. Foster, X. Jiang, and P. Dayton, Sensors **14**, 20825 (2014).
[22]E. Cherin, J. Yin, A. Forbrich, C. White, P. A. Dayton, F. S. Foster, and C. E. M. Démoré, Ultrasound Med. Biol. **45**, 2525 (2019).
[23]I. G. Newsome, T. M. Kierski, C. Carnevale, F. Visualsonics, E. Cherin, and F. S. Foster, in Proceedings of the IEEE International Ultrasonics Symposium (2019), p. 1941.
[24]K. Christensen-Jeffries, O. Couture, P. A. Dayton, Y. C. Eldar, K. Hynynen, F. Kiessling, M. O'Reilly, G. F. Pinton, G. Schmitz, M. X. Tang, M. Tanter, and R. J. G. van Sloun, Ultrasound Med. Biol. **46**, 865 (2020).
[25]S. T. Hess, T. P. K. Girirajan, and M. D. Mason, Biophys. J. **91**, 4258 (2006).
[26]C. Errico, J. Pierre, S. Pezet, Y. Desailly, Z. Lenkei, O. Couture, and M. Tanter, Nature **527**, 499 (2015).
[27]F. Lin, S. E. Shelton, D. Espíndola, J. D. Rojas, G. Pinton, and P. A. Dayton, Theranostics **7**, 196 (2017).
[28]P. Song, J. D. Trzasko, A. Manduca, R. Huang, R. Kadirvel, D. F. Kallmes, and S. Chen, IEEE Trans. Ultrason., Ferroelectr., Freq. Control **65**, 149 (2018).
[29]J.-J. Hwang and D. H. Simpson, U.S. patent 5,951,478 (1999).
[30]G. A. Brock-Fisher, M. D. Poland, and P. G. Rafter, U.S. patent 5,577,505 (1996).
[31]P. J. Phillips, in Proceedings of the IEEE Ultrasonics Symposium (2001), Vol. 2, p. 1739.
[32]K. C. Jeffries, S. Harput, J. Brown, C. Dunsby, P. Aljabar, M. X. Tang, and R. Eckersley, in IEEE International Ultrasonics Symposium (2017), Vol. 64, p. 1644.
[33]B. Heiles, M. Correia, V. Hingot, M. Pernot, J. Provost, M. Tanter, and O. Couture, IEEE Trans. Med. Imaging **38**, 2005 (2019).
[34]S. Harput, P. Tortoli, R. J. Eckersley, C. Dunsby, M. X. Tang, K. Christensen-Jeffries, A. Ramalli, J. Brown, J. Zhu, G. Zhang, C. H. Leow, M. Toulemonde, and E. Boni, IEEE Trans. Ultrason. Ferroelectr. Freq. Control **67**, 269 (2020).
[35]T. L. Christiansen, M. F. Rasmussen, J. P. Bagge, L. N. Moesner, J. A. Jensen, and E. V. Thomsen, IEEE Trans. Ultrason., Ferroelectr., Freq. Control **62**, 959 (2015).
[36]J. Foiret, H. Zhang, T. Ilovitsh, L. Mahakian, S. Tam, and K. W. Ferrara, Sci. Rep. **7**, 13662 (2017).
[37]T. M. Kierski, D. Espíndola, I. G. Newsome, E. Cherin, J. Yin, F. S. Foster, C. E. M. Demore, G. F. Pinton, and P. A. Dayton, IEEE Trans. Ultrason., Ferroelectr., Freq. Control **67**, 1 (2020).
[38]V. Hingot, C. Errico, M. Tanter, and O. Couture, Ultrasonics **77**, 17 (2017).
[39]S. Harput, K. Christensen-Jeffries, J. Brown, Y. Li, K. J. Williams, A. H. Davies, R. J. Eckersley, C. Dunsby, and M. X. Tang, IEEE Trans. Ultrason., Ferroelectr., Freq. Control **65**, 803 (2018).
[40]B. Fagrell, A. Fronek, and M. Intaglietta, Am. J. Physiol. - Hear. Circ. Physiol. **233**, 318 (1977).
[41]C. G. Caro, T. J. Pedley, R. C. Schroter, and W. A. Seed, *The Mechanics of the Circulation* (Cambridge University Press, 2012).
[42]Y. Desailly, J. Pierre, O. Couture, and M. Tanter, Phys. Med. Biol. **60**, 8723 (2015).
[43]M. Toi, Y. Asao, Y. Matsumoto, H. Sekiguchi, A. Yoshikawa, M. Takada, M. Kataoka, T. Endo, N. Kawaguchi-Sakita, M. Kawashima, E. Fakhrejahani, S. Kanao, I. Yamaga, Y. Nakayama, M. Tokiwa, M. Torii, T. Yagi, T. Sakurai, K. Togashi, and T. Shiina, Sci. Rep. **7**, 41970 (2017).
[44]M. Jeon, J. Kim, and C. Kim, Med. Biol. Eng. Comput. **54**, 283 (2016).
[45]R. F. Spaide, J. G. Fujimoto, N. K. Waheed, S. R. Sadda, and G. Staurenghi, Prog. Retinal Eye Res. **64**, 1 (2018).
[46]G. Figueiredo, C. Brockmann, H. Boll, M. Heilmann, S. J. Schambach, T. Fiebig, M. Kramer, C. Groden, and M. A. Brockmann, Clin. Neuroradiol. **22**, 21 (2012).
[47]R. C. Gessner, S. R. Aylward, and P. A. Dayton, Radiology **264**, 733 (2012).
[48]B. D. Lindsey, J. D. Rojas, K. H. Martin, S. E. Shelton, and P. A. Dayton, in IEEE International Ultrasonics Symposium (2014), Vol. 61, p. 1774.
[49]R. J. G. van Sloun, R. Cohen, and Y. C. Eldar, Proc. IEEE **108**, 11 (2020).
[50]D. Xiao, B. Y. S. Yiu, A. J. Y. Chee, and A. C. H. Yu, in *Image Analysis and Recognition*, edited by F. Karray, A. Campilho, and A. Yu (Springer International Publishing, Cham, 2019), pp. 442–451.